# ANALYSIS OF FLOODING DIRECTIONS OF THE 2011 EARTHQUAKE TOHOKU TSUNAMI

Hiroshi SANUKI[1], Tomohiro TAKAGAWA[2], Yoshimitsu TAJIMA[1] and Shinji SATO[1]

In contrast to many post-tsunami studies focusing on tsunami inundation heights, this study focuses mainly on tsunami flooding flow directions, which may have more direct impact on damages of structures. Based on tilted poles and trees in the inundated area, this study collected data of tsunami flow directions at Rikuzen-takata, Ootsuchi, and Naraha on the east coast of Japan. Numerical tsunami inundation model was then applied to each of these sites to investigate the relationship between simulated time-varying flow patterns and observed flow directions. Such link is essentially important to deepen our understandings on the dynamics of the inundation tsunami flow.

*Keywords: 2011 Tohoku Tsunami; Numerical Simulation; Flow Direction; Rikuzen-takata; Ootsuchi; Naraha*

## INTRODUCTION

The 2011 Tohoku tsunami has caused serious damages along the Japanese coast. Above all, the Sanriku coastal area, the northeast of the Tohoku region, was severely damaged by the tsunami, which showed complicated behaviors on the low area located inner of a bay with a indented coastline. This indicates that it is important to understand detailed behaviors of tsunami flooding for more effective tsunami mitigation plan.

Many investigations and studies have been conducted since the great earthquake (e.g., The 2011 Tohoku Earthquake Tsunami Joint Survey Group, 2011). The most of the reports mainly discuss the inundation height and the run-up height. On the other hand, there are a few video image-based studies which directly analyze the dynamics of the tsunami flow (e.g., Yamanaka et al., 2012). However, that is a rare case because a quality video footage is not always available.

In this study, we focused on tsunami flooding directions to study the tsunami run-up process, and conducted a field survey to find the flood traces left by the tsunami. We also carried out numerical simulation to clarify the behavior of the tsunami in coastal low area by careful comparison with the observed flow direction data.

## FIELD SURVEY

### The survey sites

Field survey were conducted at three sites as shown in Figure 1; Ootsuchi (Iwate), Rikuzen-takata (Iwate) and Naraha (Fukushima). All of the sites are the dike-enclosed low area located at the lower reach of a middle-ranged river. These sites were also significantly damaged by the 2011 Tohoku tsunami.
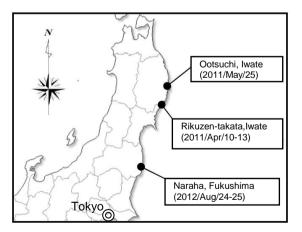


**Figure 1. The survey sites and survey date**

[1] Dept.of Civil Eng.,The University of Tokyo, 7-3-1 Hongo, Bunkyo-ku, Tokyo, 113-8656, Japan
[2] Port and Airport Research Institute, 1-1-3 Nagase, Yokosuka, Kanagawa, 239-0826, Japan

**Measurement of flow direction and inundation height**

We assumed that the tilted poles or trees indicated of the tsunami flow direction and recorded horizontal locations and angles at various points inside the inundated area. GPS-camera equipped with an electromagnetic compass was used to record the coordinates and directions as shown in Figure 2. Figure 2 also shows the examples of pillar-shaped object we collected the direction data. However, the case as seen in Figure 3 was excluded from this measurement of flow direction because it was difficult to judge the direction.

Besides the flow directions, the tsunami inundation heights were also measured with RTK-GPS based on the height of water marks left by the tsunami on the window, house-wall and so on (Figure 4).



**Figure 2. Measurement of tsunami flow direction (left) and examples of pillar-shaped object (right)**



**Figure 3. The excluded case from measurement of flow direction**



**Figure 4. Measurement of tsunami inundation height**

**Survey result of tsunami flow direction**

Figure 5 shows the observed data of tsunami flow direction and inundation height plotted on Google image. We totally collected more than 850 points of flow direction data in the site (225 in Rikuzen-takata, 362 in Ootsuchi and 269 in Naraha).

As seen in Figure 5, while the most arrows in Ootsuchi and Naraha pointed landward due to the direct impact by the tsunami attack, the one in Rikuzen-takata were not unidirectional in the inundated area. It can be inferred that a complicated flow field is generated by the tsunami in Rikuzen-takata.
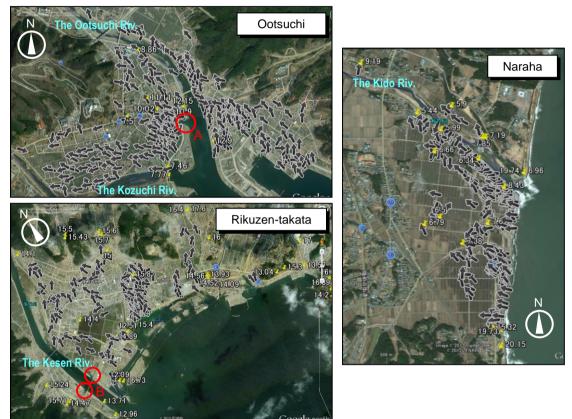


**Figure 5. The observed flow direction and inundation height (m)**

**Observation of the structural damages**

Besides measurement of the tsunami flow direction, we observed the structural damages in the inundated area. As seen in Figure 6, the breach of riverbank was found near abutment in Ootsuchi and Rikuzen-takata at the part of A and B shown in Figure 5. The collapse was also found at the bent point of left riverbank around the Kido river mouth in Naraha (Sanuki et al., 2013). Such part of riverbank will be a weak point against the tsunami because of more powerful impact.

These observations show the characteristics of the riverbank damages by the tsunami. These also suggest that the layout of the riverbank should account for the tsunami attacks mentioned above especially around the river mouth.
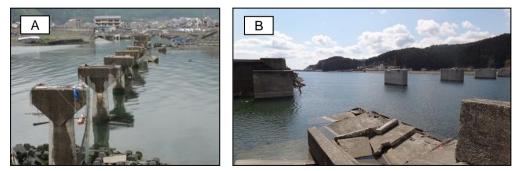


**Figure 6. Riverbank breach near abutment**

## TSUNAMI RUN-UP SIMULATION

### Basic Equations

A numerical simulation was carried out in order to investigate the tsunami dynamics in more detail. The tsunami run-up process in the river basin and the adjacent coastal plain was simulated numerically based on the nonlinear shallow water wave theory (Kotani et al., 1998).

The momentum and continuity equations are shown as follows.

$$\frac{\partial \eta}{\partial t} + \frac{\partial P}{\partial x} + \frac{\partial Q}{\partial y} = 0$$

$$\frac{\partial P}{\partial t} + \frac{\partial}{\partial x}\left(\frac{P^2}{D}\right) + \frac{\partial}{\partial y}\left(\frac{PQ}{D}\right) + gD\frac{\partial \eta}{\partial x} + \frac{gn^2}{D^{7/3}}P\sqrt{P^2 + Q^2} = 0 \qquad (1)$$

$$\frac{\partial Q}{\partial t} + \frac{\partial}{\partial x}\left(\frac{PQ}{D}\right) + \frac{\partial}{\partial y}\left(\frac{Q^2}{D}\right) + gD\frac{\partial \eta}{\partial y} + \frac{gn^2}{D^{7/3}}Q\sqrt{P^2 + Q^2} = 0$$

where, $P$, $Q$ : flux in x and y-direction, $\eta$ : water surface elevation, $D$ : total depth ($= h + \eta$), $h$ : still water depth, $g$ : acceleration of gravity, $n$ : Manning's roughness coefficient. The computation was based on the finite difference method with staggered grid.

The advection terms of momentum equations were solved with upwind difference scheme. The leap-frog scheme was applied for time-stepping.

### Computational conditions

Figure 7 are the computational domain and the topography of the site of Ootsuchi and Rikuzen-takata. Topographical data was created by the connection between laser-profiled map and sea chart. At the offshore open boundary set outside the bay mouth, the incident wave was given by the GPS-wave gauge data installed offshore of each site (Figure 8). The incident wave direction was also given as right angles to the offshore boundary. Two different Manning's roughness coefficient was given on bottom boundary. Computational conditions are listed in Table 1.

For further details of the computation for the site Naraha, refer to Sanuki et al. (2013).
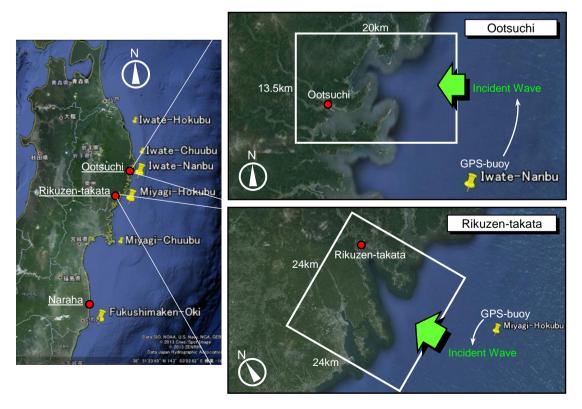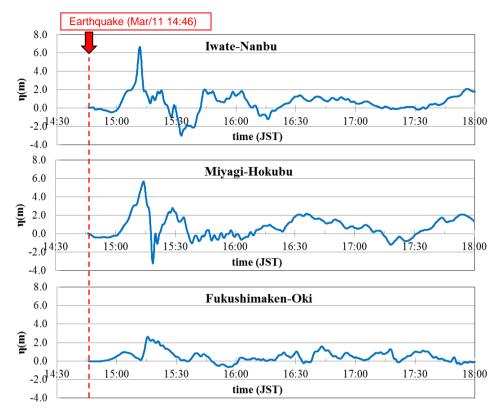


**Figure 7. Computational domains**

**Figure 8. Incident wave profile at the open boundary**

**Table 1. Computational conditions**

| The target site | Ootsuchi | Rikuzen-takata | Naraha |
|---|---|---|---|
| Computational domain | 20 x 13.5km | 24 x 24km | 10 x 15km |
| Grid size ( Δ X=ΔY) | 15m | 20m | 10m |
| Time step Δ t | 0.15s | 0.2s | 0.2s |
| Topography & Bathymetry | Offshore : Bathy-Topography Digital Data M7004 series (JHA) Onshore : Laser Profiler Data (GSI) | | |
| GPS wave buoy (PARI) | Iwate-Nanbu oki | Miyagi-Hokubu oki | Fukushimaken oki |
| Optimum coefficient | 0.90 | 1.25 | 1.40 |
| Incident wave direction | E | E30S | E18S |
| Manning's roughness coefficient | $n=0.025$ (m$^{-1/3}$s) : on seabed & riverbed $n=0.030$ (m$^{-1/3}$s) : on land | | |

**Model Verification**

We computed the tsunami flooding for 2.5 hours from the earthquake occurrence. Figure 9 are the snapshots of the computed tsunami run-up in Ootsuchi.

For the first step, the present numerical model was verified by the comparison of inundation heights (Figure 10). At each of the site, the amplitude of the incident wave was optimized with a coefficient of 0.90-1.40 (see Table 1) by the comparison of the measured and predicted inundation heights. The validity of the model was verified by good agreement shown in Figure 10.

The computed flow directions was then compared with the observed flow directions (Figure 11). Because the computation of flow directions varies by time and space, this verification compared with the flow direction at the following two timings;

1. The timing when the tsunami first arrives at survey points
2. The timing when the local flow velocity becomes the maximum

The comparisons at the timing 1 in Ootsuchi and Naraha showed good agreement. This indicates that the structures fell down at the moment when the tsunami attacked. While comparisons in Ootsuchi and Naraha showed good agreement, the one in Rikuzen-takata showed clear disagreement at both two timings.
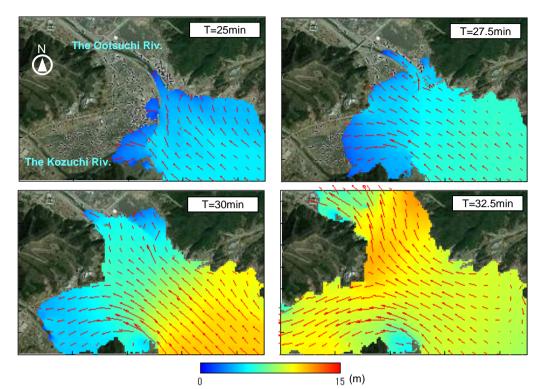
**Figure 9. Tsunami run-up simulation result for Ootsuchi (T: the time from earthquake occurrence)**
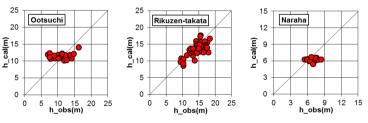


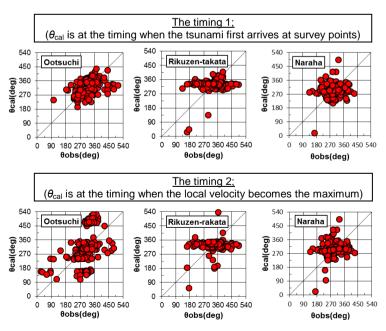**Figure 10. Comparison of inundation height**



**Figure 11. Comparison of flow direction**

## ANALYSIS OF FLOODING DIRECTIONS IN RIKUZEN-TAKATA

### The best-match timing between the computed and observed flow direction

In order to link between observed and computed flow directions in Rikuzen-Takata, we estimated the time "$t_d$", at which the computed flow direction matches best with observed one. Figure 12 shows the time variation of inundation depth, flow velocity and flow direction at the point P (see Figure 14). The time "$t_d$" is defined as the time from tsunami arrival to the maximum point of $\cos\Delta\theta$, where $\Delta\theta$ is the angle between the observed and computed flow direction. The maximum point of $\cos\Delta\theta$ means the best-match timing between the computed and observed flow direction.
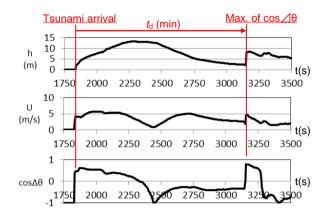
**Figure 12. Time variation at the point "P (see Figure 14)" and definition of the time "$t_d$"**

### Classification of the observed flow directions

Histogram of the estimated time "$t_d$" was then produced and shown in Figure 13. Histogram in Rikuzen-takata had two peaks; the one during the first and the other during the second tsunami floods, respectively. There are some data which corresponds to the phase during the ebb of the first tsunami.

Based on the time "$t_d$", the flow direction data was classified by flooding phase. Flooding phase was divided by two critical time; $t_d=10$ and $t_d=20$(min). Figure 14 shows the observed flow directions in arrows with different colors; blue (the first flood), red (the first ebb) and green (the second flood).

In the case of Rikuzen-takata, the relatively big second flood had different characteristics from the first flood; this is essential to classify flow direction data clearly. Because it was not the case in Ootsuchi and Naraha, the time "$t_d$" was distributed in early time range and the second peak was not so clear (Figure 13).
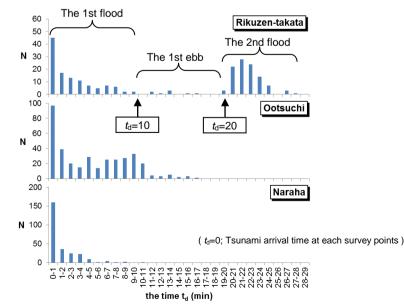
**Figure 13. Histogram of the time $t_d$**

**Figure 14. The classified flow direction data (Rikuzen-takata)**

**Comparison of tsunami flow patterns**

Numerical results were further analyzed to investigate the physical reasons; why the flow directions of the first and second flooding tsunami changed. We extracted the computed flow patterns at three different timings and compared to the observed flow directions (Figure 15).

The upper left of Figure 15 is the first flood of the tsunami run-up toward the northwest direction. This situation is seen in blue arrows in Figure 14. The second flood interacted with the first ebb flow was then forced to propagate northward (the upper right of Figure 15). Finally, the second flood was reflected at the mountain side northern steep slope and flew westward (the lower of Figure 15). These situations of the complicate tsunami flow patterns are also seen in green arrows shown in Figure 14.
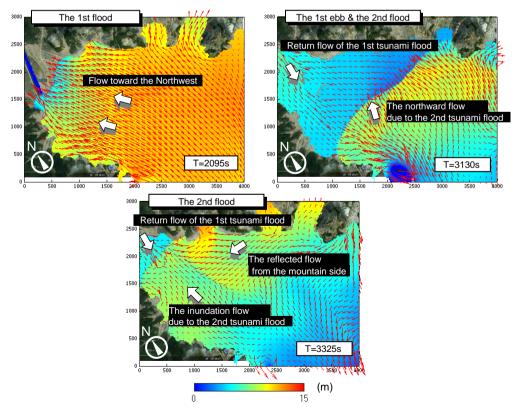


**Figure 15. Comparison of tsunami flow patterns (Rikuzen-takata)**

**CONCLUSION REMARKS**

This study investigated the dynamics of inundating tsunami characteristics based on the field measurements of the flow directions and the numerical simulation, and obtained the following conclusion remarks.

1. It was found in the field survey that most of tsunami flow directions were pointing landward due to direct impact by tsunami attack.
2. Riverbank near the abutment was found to be a weak-point against the tsunami.
3. Measured and computed flow directions were linked with each other through investigating the "best-matching" timing of tsunami inundation.
4. It was found through this analysis that the timing of dominant hydrodynamic force varies locally and flow directions of the 1st and 2nd tsunami were also different.
5. The present methodology should be helpful for better understandings of the dynamics of the inundation tsunami flow.

**REFERENCES**

The 2011 Tohoku Earthquake Tsunami Joint Survey Group. The 2011 off the Pacific coast of Tohoku Earthquake Tsunami Information (http://www.coastal.jp/tsunami2011/).

Y. Yamanaka, Y. Tajima and S. Sato. 2012. Video image-based analysis of concentrating tsunami dynamics on Shirahama beach in Ryori bay. Proceedings of Coastal Engineering, JSCE, 68:341-345.

H. Sanuki, Y. Tajima, H. Yeh and S. Sato. 2013. Dynamics of the tsunami flooding to the river basin. Proceedings of Coastal Dynamics 2013, SHOM, 317-318.

H. Sanuki, R. Takemori, Y. Tajima and S. Sato. 2013. Study on tsunami flooding in river based on video images and numerical simulation. Proceedings of Coastal Engineering, JSCE, 69:196-200.

M. Kotani, F. Imamura and N. Shuto. 1998. Tsunami Run-up Simulation and Damage Estimation by Using GIS. Proceedings of Coastal Engineering, JSCE, 45:356-360.